19F MAGNETIC RESONANCE IMAGING OF INCREASED VCAM-1 EXPRESSION IN THE KIDNEYS OF APOE-NULL MICE USING TARGETED PERFLUOROCARBON NANOPARTICLES

R. Southworth[1], J. Chen[2], L. Zhang[2], M. Kaneda[2], H. Zhang[2], and S. Wickline[2]

[1]Imaging Sciences, King's College London, London, United Kingdom, [2]C-TRAIN Group, Washington University School of Medicine, St. Louis, MO, United States

Background

Vascular Cell Adhesion Molecule-1 (VCAM-1) is responsible for the tethering of leukocytes to the vascular lumen in early inflammation. It has been implicated in the pathogenesis of numerous inflammatory diseases, and therefore represents a potentially useful molecular imaging target. We have developed unique liquid perfluorocarbon nanoparticles which can be functionalised with homing ligands in their outer lipid layer, such that they can be targeted to intravascular biomarkers of disease. They are capable of delivering a targeted payload of over 50,000 Gd atoms, or by virtue of their high ^{19}F content (98% by volume), providing a *quantifiable* ^{19}F MR signal. Here, we describe their use in specific visualisation and quantification of VCAM-1 expression in the kidneys of hyperlipidaemic ApoE$^{-/-}$ mice.

Materials and Methods

Nanoparticle formulation: Liquid PFC nanoparticles were formulated using methods previously developed in our laboratories. All emulsions contained 0.135 mol% of rhodamine in the surfactant layer. For targeted emulsions, the VCAM-1 targeting peptide (VHPKQHRGGSGC) in 6 mM EDTA was added to the lipid film at a 1:1 molar ratio of peptide to MPB-PEG-DSPE.

Experimental: ApoE$^{-/-}$ mice and C57BL6 mice received a high cholesterol diet (Harlan Teklad, Madison Wis; 0.2% Cholesterol) for 8 weeks. Mice were injected with targeted or non-targeted nanoparticles (n=6/group) via the tail vein (1µl/g). After 2 hours, mice were terminally anaesthetised, heparinised, and exsanguinated. Both kidneys were excised for subsequent analysis. One kidney was mounted in OCT medium and rapidly frozen prior to immunohistochemistry; the other was stored in saline-filled vials on ice for ^{19}F MR spectroscopy and imaging on an 11.74T Varian *UNITY*-INOVA scanner.

Results

Immunohistochemistry and fluorescence microscopy: We observed extensive staining for VCAM-1 throughout ApoE$^{-/-}$ kidney, particularly in the capillaries of the glomeruli, and the proximal and distal arterioles; in healthy wild-type, VCAM-1 staining was virtually absent (Fig 1A). Nanoparticle biodistribution within each kidney section was visualised using fluorescence microscopy, by virtue of the nanoparticles' rhodamine content. Rhodamine fluorescence was clearly visible in the capillaries of the glomerulus and the afferent and efferent arterioles of ApoE$^{-/-}$ kidneys, while very little was present around the glomeruli of control kidneys (Fig 1B).

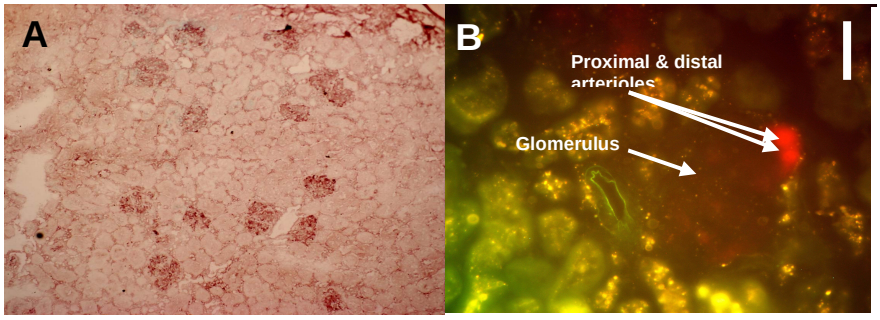

Fig 1A Representative image showing VCAM-1 immunostaining in kidney from an ApoE$^{-/-}$ mouse fed on a high-fat diet.
Fig 1B: Fluorescence micrographs showing marked fluorescence from rhodamine-labelled VCAM-1-targeted nanoparticles in ApoE kidney in proximal and distal aterioles and glomerular capillaries.

^{19}F MR Spectroscopy and imaging: VCAM-1-targeted nanoparticle accumulation was significantly higher in ApoE$^{-/-}$ kidneys than in non-ApoE$^{-/-}$ kidneys (36.55 ± 8.81 vs 15.64 ± 2.34 (targeted) and 15.41 ± 1.9 (non-targeted) x 10^8/g wet weight ($p<0.05$), and targeted nanoparticles accumulated in ApoE$^{-/-}$ kidneys to a significantly greater extent than non-targeted nanoparticles did (36.55 ± 8.81 vs 9.33 ± 2.23 x 10^8/g wet weight ($p<0.05$)). There was no significant difference between targeted and non-targeted nanoparticle uptake in kidneys from wild-type non ApoE$^{-/-}$ mice (Fig 2). VCAM-1-targeted nanoparticles were clearly visible in ^{19}F images from ApoE$^{-/-}$ mouse kidneys, but virtually absent in wild-type control mouse kidneys (Fig 3).

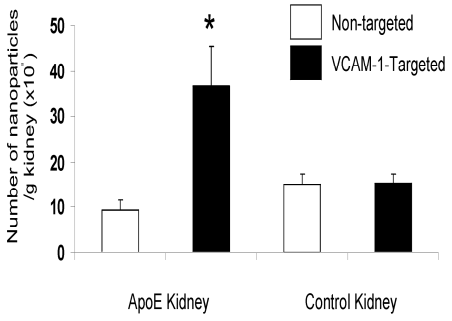

Fig 2 (left) Absolute quantification of nanoparticle targeting to VCAM in ApoE and control kidney, quantified by ^{19}F NMR spectroscopy.
Fig 3 (right): MR images of VCAM-1 targeted nanoparticle accumulation in ApoE$^{-/-}$ (top) and control (bottom) kidneys showing gross structure (^{1}H), nanoparticle distribution (^{19}F), and filtered overlay of the two images (^{1}H+^{19}F)

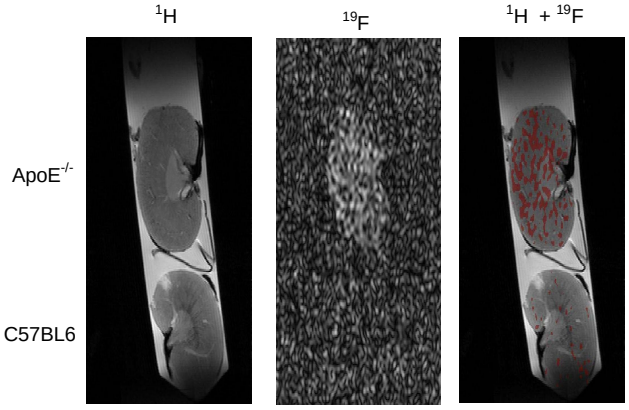

Conclusion

Perfluorocarbon nanoparticles have several advantages over existing MR-based molecular imaging probes, in that they provide "positive" contrast, have intrinsically quantifiable signals with no background signal in biological tissues, and have the potential to simultaneously track different biological processes by chemical shift imaging of different perfluorocarbon cores. Here, we describe the first successful application of VCAM-1-targeted perfluorocarbon nanoparticles for MR-based imaging of renal pathology.